Applied Thermal Engineering 106 (2016) 1209–1216

Contents lists available at ScienceDirect

Applied Thermal Engineering

journal homepage: www.elsevier.com/locate/apthermeng

Research Paper

Heat transfer enhancement of a heat source located in a wake zone using rectangular vortex generators

R.K. Ali

Benha University, Faculty of Engineering Shoubra, Mechanical Engineering Department, 108 Shoubra Street, Cairo 11689, Egypt

HIGHLIGHTS

- Heat transfer enhancement of electric device or electronic module near a wake region was investigated.
- The effect of position, attack angle and size of vortex generator (VG) were presented.
- Nu_L of the downstream heat source with VGs can be enhanced by 14.5% within $4676 \leqslant Re_L \leqslant 12{,}929$.
- An insignificant increase of 10% in the friction factor with applying VGs was noticed.

ARTICLE INFO

Article history:
Received 23 March 2016
Revised 25 May 2016
Accepted 9 June 2016
Available online 10 June 2016

Keywords:
Vortex generator
Heat transfer enhancement
Pressure drop
Experimental

ABSTRACT

This study investigated experimentally the effect of rectangular winglet vortex generators on thermal performance of square flat heat source near a wake region. Rectangular winglets were fixed on the base board with common inflow orientation to direct the flow toward the core of stagnation zone. The proposed configuration causes significant flow acceleration that enhances heat transfer from near-wake heat source surfaces besides the generated large-scale turbulence vortices. Over Reynolds number range of $4200 \leqslant Re_L \leqslant 12{,}300$, vortex generators with height ratio (b/B) of 3/4–3/2 and length ratio (a/S) of 1/3–2/3 at attack angle of $\alpha = 45^\circ$ exhibit better thermal performance. Downstream and spanwise distances of $x = (1/3–2/3)S$ and $y = (2/10–3/10)L$ have the largest heat transfer enhancement, respectively. The heat transfer was augmented such Nu_L of the downstream heat source exceeds Nu_L of single heat source by values reach 9.1% at $Re_L = 4676$ with applying vortex generator strategy. For physical situation of two rows, Nu_L of the downstream heat source with installing rectangular winglets vortex generators can be enhanced by 14.5% within $4676 \leqslant Re_L \leqslant 12{,}929$ at $X = 10/50$, $Y = 10/50$ and $\alpha = 45^\circ$. An insignificant increase in the friction factor of 9.7% over $12{,}135 \leqslant Re_{Dh} \leqslant 34{,}305$ was noticed.

1. Introduction

Since the advent of the transistor and integrated circuit, the performance of electronic equipment has increased significantly while system packaging continues to decrease. Multi-chip modules can provide much higher packaging efficiency that improves the system electrical performance and reduces weight and costs [1–3].

Sedney [4] introduced a review of the effects of small protuberances on the boundary layer flows. A system of horseshoe vortices forms on both sides and a wake region downstream the protuberance as shown in Fig. 1. Both legs of the horseshoe vortex system form a pair of counter rotating streamwise vortices. Also, Incropera [5], Sathe and Sammakia [6] and Bergles [7] introduced a review of evolution of electronics cooling techniques from a historical perspective. From this review, it appears that such data is not sufficient especially at high Reynolds numbers. Culham et al. [8] analytically explored the thermal wake phenomena. It was shown that the thermal wake is a significant contributor to the temperature rise of the downstream element, if the element was located within a certain distance of the upstream element. The most significant heating effects were seen when the element spacing was of one element length. Faghri et al. [9] introduced flow visualization over parallel circuit board populated with uniform protruding rectangular blocks. Flow visualization illustrated that the boundary layer is separated as it passed over the first row and reattached downstream. Separation bubbles are formed on the top surfaces of the blocks in the first row, and recirculation flow is obtained between blocks. Wirtz [10] found similar results in another experimental study.

Sparrow et al. [11,12] experimentally investigated the effect of implemented barriers in arrays of rectangular modules and

E-mail addresses: Ragabkhalil1971@gmail.com, Ragab.aboyazid@feng.bu.edu.eg

http://dx.doi.org/10.1016/j.applthermaleng.2016.06.062
1359-4311/

Nomenclature

Symbols

A	surface area, m^2
a	vortex generator length, m
B	heat source height, m
b	vortex generator height, m
D	diameter, m
H	channel height, m
h	heat transfer coefficient, W/m^2 K
k	thermal conductivity of the fluid, W/m^2 k
L	heat source length, m
P	power, W
Δp	pressure drop, Pa
Q	heat transfer rate, W
q	heat flux, W/m^2
R	resistance, Ω
S	separation distance, m
T	temperature, K
V	volt, V
v	mean velocity, m/s
X	dimensionless downstream distance
x	downstream distance, m
Y	dimensionless spanwise distance
y	spanwise distance, m

Greek letters

Δ	drop ratio in the average Nusselt number
ρ	density, kg/m^3
v	kinematic viscosity, m^2/s

Subscript

A	inlet fluid
average	average
Cond	heat lost by conduction
D_h	based on hydraulic diameter
f, inlet	fluid inlet
F	fluid
Input	input
L	based on the heat source length
Net	net heat transferred to fluid
Rad	heat lost by radiation
smooth duct	refers to flow in smooth duct
single	single heat
s	surface

Dimensionless terms

f	friction factor, $f = \frac{2\Delta p*(D_h/L)}{\rho v^2}$
Nu_L	average Nusselt number, $Nu_L = \frac{hL}{k_f}$
Re_L	Reynolds number based on heat source length, $Re_L = \frac{vL}{v}$
Re_{Dh}	Reynolds number based duct hydraulic diameter, $Re_{Dh} = \frac{vD_h}{v}$
X	dimensionless downstream distance, $X = \frac{x}{L}$
Y	dimensionless spanwise distance, $Y = \frac{y}{L}$

reported that a significant improvement in the heat transfer coefficient of the module downstream the barrier. Ratts et al. [13] and Karniadakis et al. [14] investigated the heat transfer enhancement by placing eddy promoter cylinders in a grooved-channel flow. They found enhancement in the forced convective heat transfer coefficient up to 82% when cylinders were placed periodically above the back edge row of chips. Chou and Lee [15] and Wu et al. [16] investigated the unsteady flow and heat transfer characteristics of rectangular sources with vortex generation from a rectangular plate on the top of a down-stream chip. The results show that the installation of an inclined plate above an upstream heat source results in a periodically unsteady flow and it can effectively enhance the heat transfer performance. Ali [17] investigated experimentally the heat transfer enhancement by perforation the stagnation zone base between two rectangular heat sources with separation distance ratio (S/L) of 0.5 and 1.0. The perforation area ratio was of 0, 0.0736, 0.1472 and 0.2944. It was observed that perforation enhances the heat transfer coefficients and reduces the module temperature significantly. Also, Ali [18] studied experimentally the heat transfer from a heat source simulating an electronic chip mounted on a printed circuit board placed downstream of a guide fence at $5000 < Re_L < 30{,}000$. Correlations for the average Nusselt number were obtained as a function of Reynolds number, the guide fence height and separation distance. Luviano-Ortiz et al. [19] and Herman and Kang [20,21] investigated the enhancement of grooved channel with curved deflectors or cylindrical eddy promoters. They showed that the increase in the heat transfer coefficient is due primarily to the fluid motion stirred in the area between the heated block but this implementation also increases the pressure drop in the channel. Cylinders and deflectors enhance heat transfer in the grooved channels factor of 1.2–1.8 and 1.5–3.5, respectively when compared with basic grooved as presented by Herman and Kang [20,21]. Vortex generators (VGs) are considered as a passive heat transfer enhancing technique which are attached to boundaries and protrude into the flow at an angle of attack to the flow direction. The basic role of vortex generators (VGs) is to induce secondary flow which disturbs the thermal boundary layer development. The generated longitudinal vortices help removing the heat from the wall to the core of the flow by means of large-scale turbulence [22]. Different VGs shapes were investigated to introduce the effect on the thermal performance of heat exchangers [23–27]. Jacobi and Shah [27] introduced a review of heat transfer enhancement through the use of longitudinal vortices from vortex generators shown in Fig. 2.

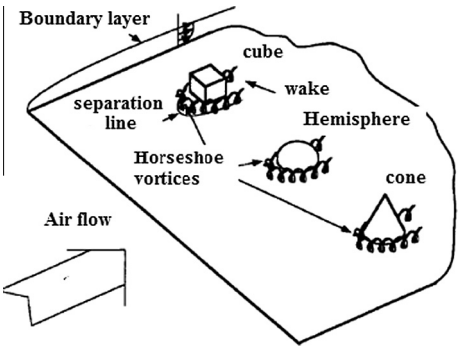

Fig. 1. Effects of small protuberances on the boundary layer flows [4].

This review showed that the applications of vortices generators in heat exchangers as an enhancement technique is promise, but a deeper understanding of the flow and heat transfer interactions is needed to identify promising implementations for specific applications. Chomdee and Kiatsiriroat [28] presented an experimental investigation on heat transfer enhancement using delta winglet type vortex generators with attack angles of 10°, 15° and 20° for air cooling in the entrance region of an in-line array of electronic modules. From the available literature, it is shown that the pres-

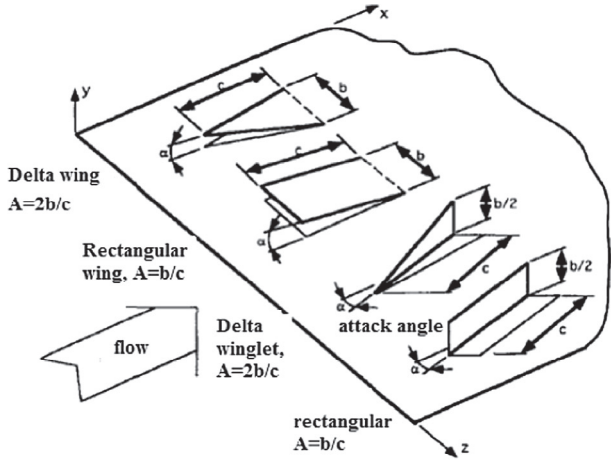

(a) Common vortex generators and associated dimensions

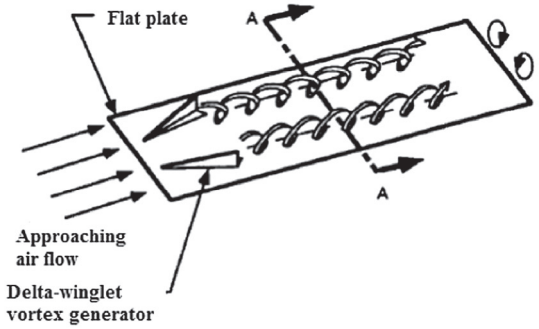

(b) common inflow configuration

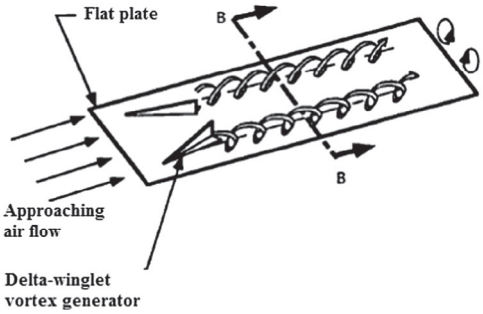

(c) common outflow configuration

Fig. 2. Vortex generators shapes and configurations [27].

ence of a heat source in a wake region decreases heat transfer rate and elevates the form drag. The main objective of the present research is to propose vortex generators strategy that can augment heat transfer and monitor the associated pressure drop for a heat source located in the wake zone of another upstream one. The proposed strategy is to place a pair or more of rectangular winglets over the common velocity range in electronic components cooling. An experimental setup was fabricated to explore the effect of position, attack angle and the size of vortex generator on thermal performance of the downstream heat source. The dimensions of the heat source, heater capacity and the air velocity were select to simulate a real case which is applied in cooling of electronic module.

2. Experimental apparatus

The experimental facility employed in the present work is a wind tunnel oriented horizontally as shown in Fig. 3. It consists of centrifugal blower, orifice meter, entrance duct, test section and instrumentations to measure temperature, air flow rate and electrical power input. A centrifugal type air blower of 225 mm inlet section diameter driven by an AC motor of 1.5 hp is used to induce the required flow rate. The flow rate is controlled at the outlet of the blower via a variable area outlet gate. A plexiglass horizontal duct of 200 mm width, 100 mm height (H) and 2500 mm length is used as an entrance length. The centrifugal blower and the dimensions of the air duct are selected to give mean flow velocity from 1.89 to 4 m/s that representative for flow velocity in electronic cooling applications. The test section consists of a heat source placed downstream dummy block of the same size which are mounted firmly on circuit board plate as shown in Fig. 4. The gap between the heat source and the dummy block (S) is 30 mm. The dimensions of the heat source is selected to simulate short flat electronic module like flat packs introduced in Wirtz and Dykshoorn [29] and Sparrow et al. [30]. The heat source is fabricated from a hollow rectangular aluminum block and measured 50 mm × 50 mm with 10 mm height (B) with inserted heating element. The thickness of vertical sides and the upper surface is 5 mm. Nickel chromium heating wire of 0.5 mm diameter is wrapped uniformly around a mica sheet which is sandwiched between two sheets and inserted inside the hollow aluminum block. The input power to the heater is regulated using 0.5 kW AC transformer such that the heat dissipated is 5 W. The dimensions of the heat source combined with the heat dissipated gives a heat flux of order 1300–1400 W/m^2 which is reasonable for electronic module without heat sink. Five pre-calibrated thermocouples made of copper constantan wires of 0.2 mm diameter are embedded in grooves machined in the internal surfaces of aluminum block as shown in Fig. 5. The back surface of the heat source is insulated with 5 cm asbestos layers where two thermocouples are embedded to estimate the back conduction heat loss. The inlet fluid temperature was measured by a thermocouple located at the wind tunnel center before the dummy block. A digital differential manometer with accuracy of 1 Pa is used to measure the pressure drop across the test section and the orifice meter. The thermocouples were connected to fifteen channels data acquisition system to record the temperatures.

A pair of rectangular winglet made of 0.5 mm thick galvanized steel is used to direct the flow toward the stagnation zone. The present configuration of the rectangular winglet is common inflow orientation with spanwise distance between the trailing edges is wider than the leading edges, as shown in Fig. 6. The different configurations and the investigated parameters related to the vortex generators are presented in Table 1. Reynolds number is ranged from 4000 to 12,000 covering the transitional and turbulent region.

3. Test procedure and data reduction

After VG pair is installed at a specific location, the blower and transformer are switched on such that the air flow rate and applied voltage are adjusted to the required values. The readings of all thermocouples are recorded by using data acquisition system every second. A steady state condition is considered to be achieved when the reading of thermocouples embedded in the insulation remain steady within 1.0 °C for 15 min. The operating parameters are then recorded including all temperatures, orifice head, applied voltage and pressure drop across the test section. The air flow rate is changed six times such that $4200 \leqslant Re_L \leqslant 12{,}300$ for each position. The above procedures are repeated for other positions and orientations of each VG pair. The different investigated configurations are shown in Table 1.

The input electrical power to the heat sources is corrected for back conduction loss as,

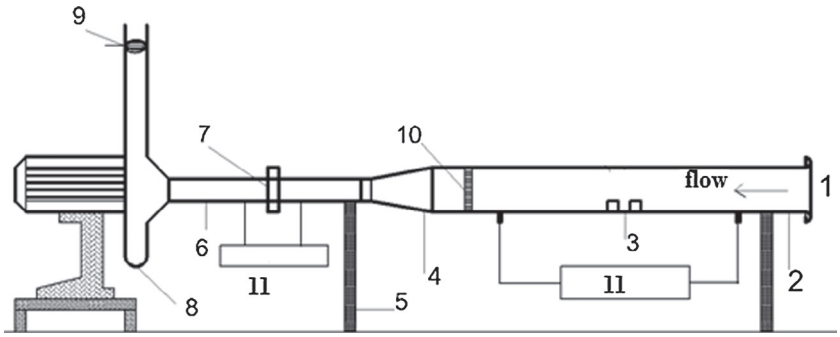

1- Bell mouth 2-Entrance Length 3- Test Section 4-Transition Duct

5- Steel Stand 6–connecting pipe 3" 7- Orifice Meter 8- Air Blower

9- Discharge Gate 10-Straightener 11- digital manometer

Fig. 3. Experimental apparatus.

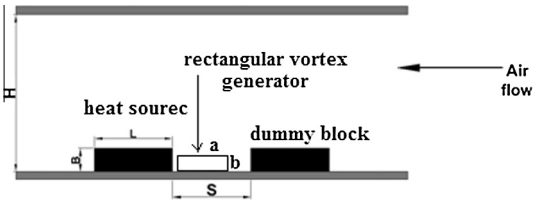

Fig. 4. Front view of the test section.

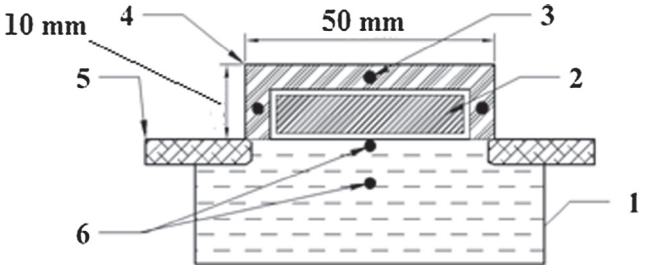

1- Asbestos insulation 2- Electric heater 3-thermocouples 4-square heat source

5- base board 6-insulation thermocouples (z_{ins} = 13mm)

Fig. 5. Details of the heat source.

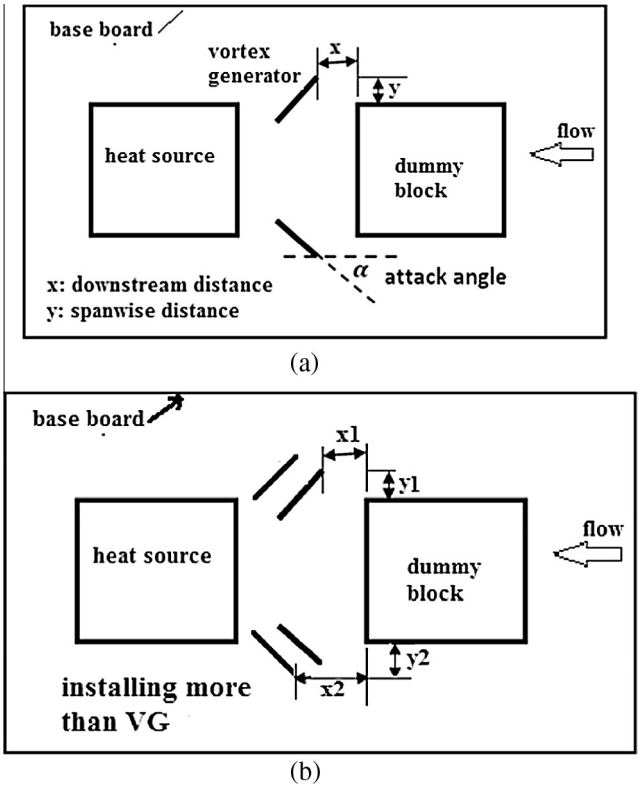

Fig. 6. Top view of test section: (a) single pair of VG (b) two pairs of VG (G1 and G2 in Table 1).

$$Q_{net} = Power_{input} - Q_{cond} \quad (1)$$

The input power to the heater ($Power_{input}$) is regulated with 0.5 kW AC transformer and can be calculate from $(V^2/R)\cos\varphi$). The AC power factor ($\cos\varphi$) is assumed to be 0.95. The conduction loss across the asbestos layers is estimated from;

$$Q_{cond} = \frac{k_{ins}A_{ins}(T_{i,ins} - T_{o,ins})}{z_{ins}} \quad (2)$$

where $T_{i,ins}$ and $T_{o,ins}$ are the temperature of the thermocouples embedded inside insulation. A_{ins} and Z_{ins} are insulated back area and distance between embedded thermocouples, respectively. In all experiments, the conduction loss does not exceed 10% of the input electrical power.

The results are presented in terms of the convective heat transfer coefficient, h, Nusselt number and fanning friction factor as;

$$h = \frac{q}{T_{average} - T_{f,inlet}} \quad (3)$$

where $T_{average}$ and $T_{f,inlet}$ are the average temperature of heat source surfaces ($T_{average} = \sum T_{surface}/5$) and inlet fluid temperature, respectively. The applied heat flux (q) on the internal surface of the tube is calculated from ($q = Q_{net}/A_s$).

The experimental results are presented in dimensionless form. The definition of Nusselt and Reynolds numbers and friction factor can be calculated from relation;

$$Nu_L = \frac{hL}{k_f} \quad (4)$$

Reynolds number based on heat source length is calculated using average velocity as;

$$Re_L = \frac{vL}{\nu} \quad (5)$$

Table 1
Vortex generator configurations.

Configuration	Dimensions, mm	Attack angle, α	Spanwise distance, y (mm)	Downstream distance, x (mm)	Runs
VG1	a = 15 mm b = 5 mm	45°	10	10	6
VG2	a = 15 mm b = 7.5 mm	15°, 30°, 45° and 60°	5, 10, 15 and 20	0, 10 and 20	288
VG3	a = 15 mm b = 10 mm	45°	10	10	6
VG4	a = 20 mm b = 10 mm	45°	10	10	6
VG5	a = 20 mm b = 15 mm	45°	10	10	6
VG6	a = 15 mm b = 15 mm	45°	10	10	6
G1	VG3 VG5	45°	y1 = 5 y2 = 17	x1 = 8 x2 = 12	6
G2	VG2 VG5	45°	y1 = 10 y2 = 18	x1 = 10 x2 = 16	6

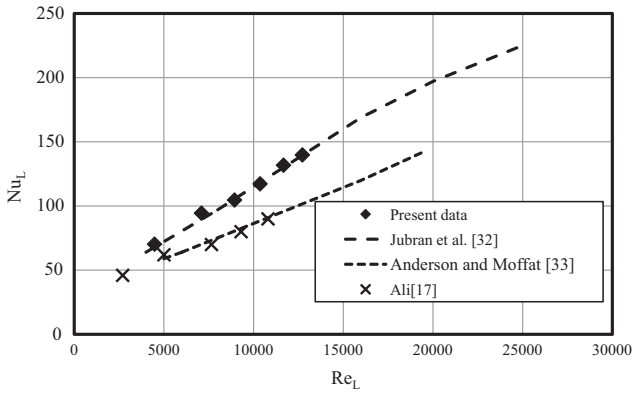

Fig. 7. Validation of the experimental Nusselt number for single heat source (without dummy block or VGs).

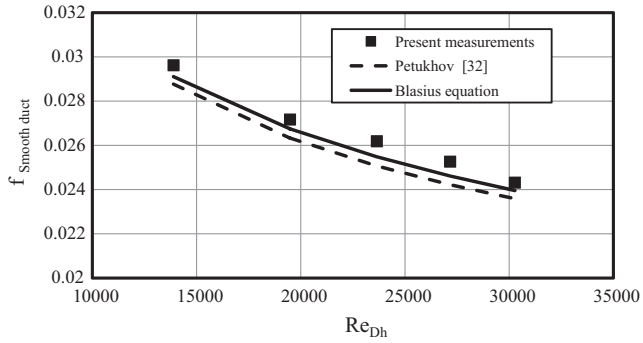

Fig. 8. Validation of the experimental Fanning friction factor for smooth duct.

The friction factor is calculated from the following relation;

$$f_c = \frac{2\Delta p * (D_h/L)}{\rho v^2} \quad (6)$$

The uncertainty of experimental results can be analyzed based on accuracy data of individual transducers and measuring techniques. It is calculated based upon the root sum square combination of the effects of the individual inputs appear in Eqs. (1)–(6) as introduced by Kline and McClintock [31]. The maximum uncertainties in Reynolds number, *Nu* and Fanning friction factor are 2.7%, 5.8% and 7.5% at lower limit of Reynolds number (Re_L = 4200).

4. Experimental results and discussion

4.1. Validation of setup and measurements

For the validation of the experimental setup and measuring techniques, the present Nusselt number for a single heat source is compared with the experimental data Jubran et al. [32], Anderson and Moffat [33] and Ali [17] as shown in Fig. 7.

Also the obtained results for friction factor in turbulent flow in smooth duct are compared with the correlations of Petukhov [34] and Blasius equation cited in [35] as shown in Fig. 8.

$$f = (0.79 Ln Re_{Dh} - 1.64)^{-2} \quad (7)$$

$$f = 0.316 Re_{Dh}^{-0.25} \quad (8)$$

The maximum error between the present measurements of friction factor and the correlated values of Petukhov [34] is 7.1% as shown in Fig. 8. This good agreement in Nusselt number and pressure drop comparisons reveals the accuracy of the experimental setup and measurement technique.

4.2. Heat transfer results

Previous studies have demonstrated that the heat transfer along a channel with periodic insertion of heated blocks is low due to the stagnation of the flow in regions located between consecutive blocks and the formed boundary layer as presented in [8–10,32]. The increase in the heat transfer in this type of channel depends largely on propelling the flow toward this region and disturbing the formed thermal boundary layer as discussed [12–21]. The present study aims to apply propelling flow strategy toward the recirculation zone between the heated blocks that simulating the electronic modules using VGs. Fig. 9 illustrates the effect of presence of VG2 on the average temperature downstream heat source within $1.35 < V_{average} < 4.2$ at X = 10/50. The experimental data presented in Fig. 9 is carried at a nearly equal ambient temperature (26–27 °C) and the same feeding voltage to the heating element (10.1–10.4 V) at three different attack angles. In general, it can be seen that installing VGs reduces the average temperature of downstream heat source and its effect is attractive at $\alpha = 45°$ and Y = 10/50. It is convenient to introduce the effect of VGs in the average Nusselt number of the downstream heat source as shown in Figs. 10–12 to avoid the influence of ambient temperature and internal rate of heat generation changes. The investigated streamwise distance ($X = x/L$) are 0/50, 10/50 and 20/50 while spanwise distance ($Y = y/L$) are 5/50, 10/50, 15/50 and 20/50. The attack

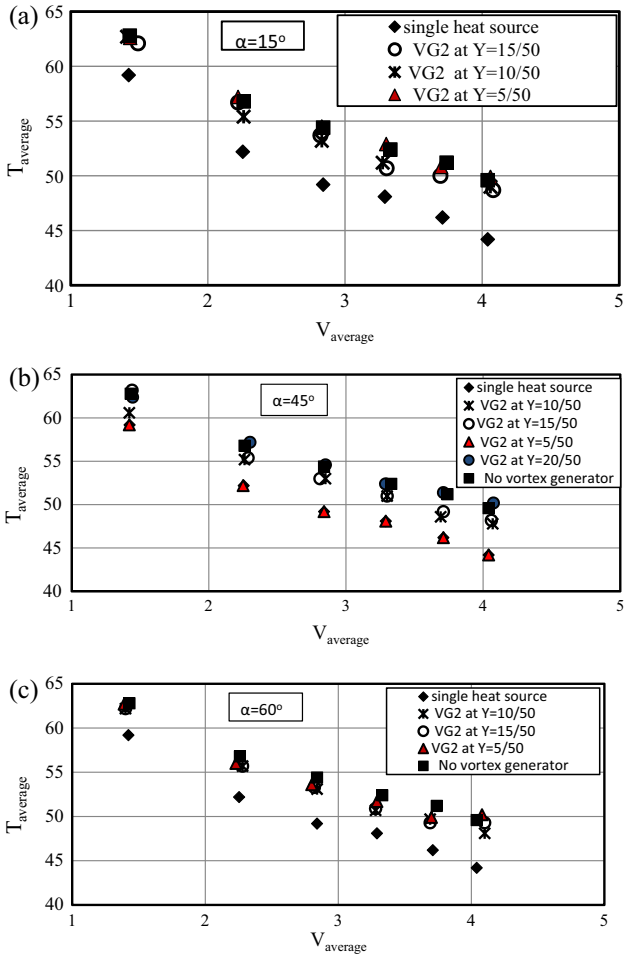

Fig. 9. Effect of vortex generator spanwise distance on average temperature of the downstream heat source for VG2 and $x/L = 10/50$: (a) $\alpha = 15°$, (b) $\alpha = 45°$, and (c) $\alpha = 60°$.

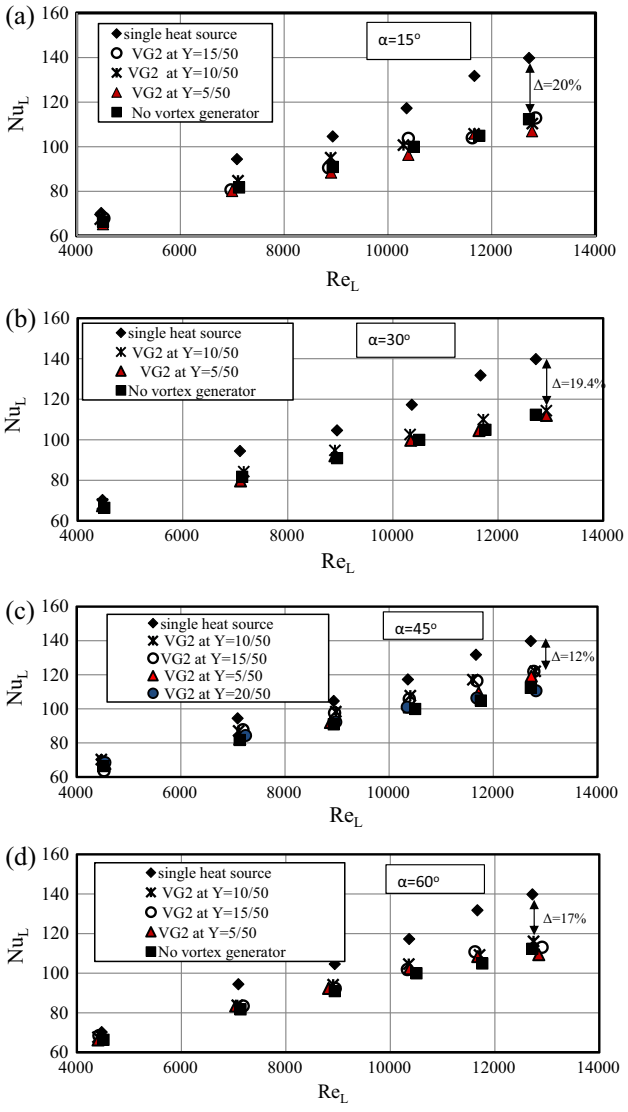

Fig. 10. Effect of vortex generator spanwise distance on average Nussult number of the downstream heat source for VG2 and $x/L = 10/50$: (a) $\alpha = 15°$, (b) $\alpha = 30°$, (c) $\alpha = 45°$, and (d) $\alpha = 60°$. ($\Delta = (Nu_{single\ heat\ source} - Nu_{downstream\ heat\ source})/Nu_{single\ heat\ source}$).

angles are varied as $\alpha = 15°$, 30°, 45° and 60°. As shown in Figs. 10–12, the drop ratio in the average Nusselt number of the downstream heat source (Δ) at a separation distance (S/L) of 30/50 reaches 20% at Re_L = 12,718. By examining Figs. 10–12, it is noticed the locating the vortex generator at $X = 10/50$ and $Y = 10/50$ with attack angle $\alpha = 45°$ has the largest heat transfer enhancement. At $Re_L = 4507.9$, the rectangular winglet brings 2% increase in Nu_L of the downstream heat source over Nu_L of single heat source. Also, the drop in the average Nusselt number of downstream heat source is lowered to 12.2% compared with 20% decrease without vortex generator at Re_L = 12,718. In order to understand the physics, the vortex generator concept induces flow acceleration toward the stagnation zone between the heat sources as well as elevating turbulence level due to the generated vortices. The nozzle-like flow created by the rectangular winglet pair brings damage of the recirculation flow confined inside the stagnation zone and thereby remove the zone of poor heat transfer from the near-wake surfaces of the heat sources. This type of flow structure has been confirmed by visualizing the flow by means of particle image velocimetry (PIV) [36] and the review presented by Jacobi and Shah [27].

Fig. 10 indicates a negligible effect for VG at spanwise distance greater than $Y = 10/50$ with small attack angles 15° and 30°. This can be returned to the flow would not reach stagnation region and its effect is limited to generated longitudinal vortices passed over the sides of the downstream heat source as shown in Fig. 2. Also, installing the vortex generator closer to the heat sources (at $Y = 5/50$ in Fig. 10) for all attack angles may exhibit negative effect. This is due to the presence of the winglet in the vicinity of the wake region confined by the horseshoe vortices generated by the upstream block as presented in the review of Jacobi and Shah [27] and shown in Fig. 1. As shown in Fig. 11, locating the vortex generator at later downstream distance ($X = 10/50$ and $20/50$) provides higher enhancement effect (drop in Nu_L is decreased from 20% to 12.2%) than $X = 0/50$ at $\alpha = 45°$. This is because a downstream distance of X = 10/50 directs the flow to the core of the stagnation zone and consequentially damage the recirculation flow beside enhancing the turbulence level on surfaces of downstream heat source. The generated large scale turbulence vortices stand behind the enhancement in Nu_L of at $X = 20/50$. As mentioned previously and shown in Fig. 12, the attack angle of $\alpha = 45°$ brings the best enhancement due directing the flow to the core of stagnation zone and elevating the turbulence level on the downstream heat sources. It can be concluded from the above discussion that position at the mid of separation distance ($X = 10/50$) and spanwise distance ($Y = 10/50$) with attack angle of $\alpha = 45°$ has the better effect

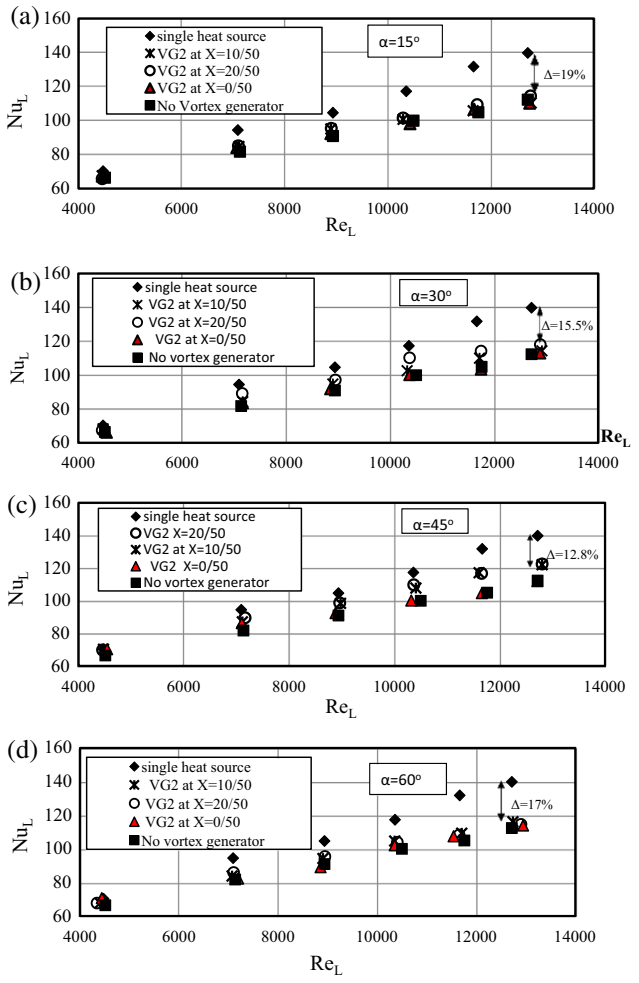

Fig. 11. Effect of vortex generator downstream distance on average Nussult number of the downstream heat source for VG2 and *y*/*L* = *10/50*: (a) $\alpha = 15°$, (b) $\alpha = 30°$, (c) $\alpha = 45°$, and (d) $\alpha = 60°$.

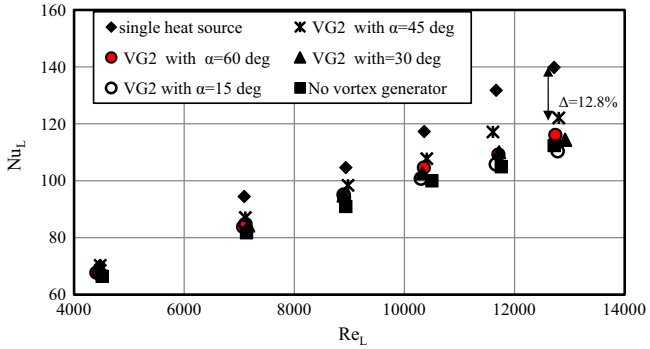

Fig. 12. Effect of attack angle on average Nussult number of the downstream heat source at for VG2 at *Y* = *10/50* and *X* = *10/50*.

on the downstream heat source Nusselt number. Fig. 13 shows the effect of size and number of vortex generators on average Nusselt number and friction factor at *X* = *10/50, Y* = *10/50* and $\alpha = 45°$. It can be seen applying single rectangular winglet with height ratio of 0.75 to 1.5 and groups (G1 and G2) regains and exceeds Nu_{single} at $Re_L = 4676.2$. This is due to the strong longitudinal vortices generated by vortex generator having larger area facing the air flow. It can be seen that Nu_L of the downstream heat source exceeds Nu_{single} by 9.1%, 7.1% and 4.8% when installing G2, VG5 and G1,

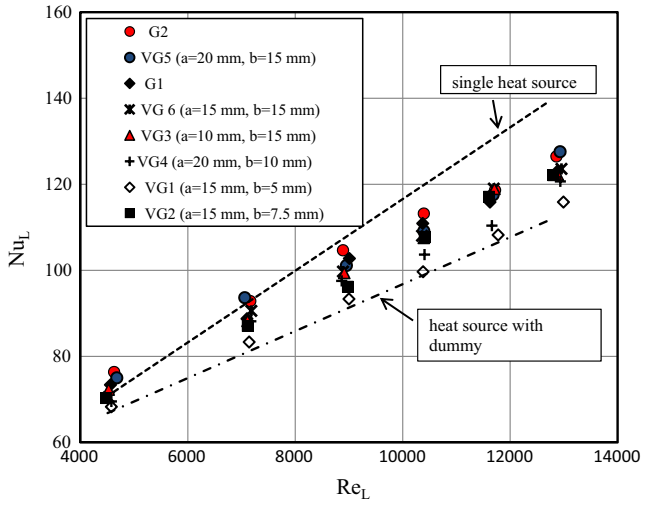

Fig. 13. Effect of size and number of vortex generators on the average Nussult number of the downstream heat source at *X* = *10/50*, *Y* = *10/50* and $\alpha = 45°$.

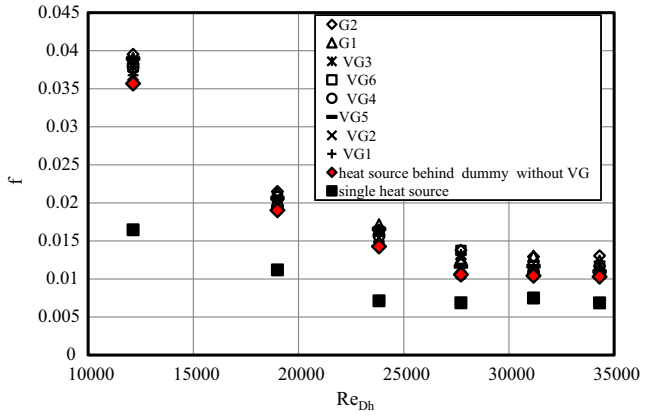

Fig. 14. Effect of size and number of vortex generators on the friction factor at *X* = *10/50*, *Y* = *10/50* and $\alpha = 45°$.

respectively. The enhancement effect decreases with increasing Reynolds number over the studied range. At $Re_L = 7058$, the effect of wake region behind the upstream block is diminished where drop in Nu_L of the downstream heat source is disappeared for G2 and VG5. Within $8887 \leqslant Re_L \leqslant 12{,}929$, the drop Nu_L of the downstream heat source with fixation G2 and VG5 is decreased to 8% compared with 20.1% drop Nu_L without vortex generator. For physical situation of two heat sources, Nu_L of the downstream heat source (with installing G2, VG5 and G1) is increased by 14.5–10% within $4676 \leqslant Re_L \leqslant 12{,}929$ at *X* = *10/50, Y* = *10/50* and $\alpha = 45°$.

4.3. Friction factor results

Fig. 14 shows the values of friction factor obtained for the applying vortex generators concept on forced convection cooling of heat sources at *X* = *10/50, Y* = *10/50* and $\alpha = 45°$. A significant pressure drop is obtained for a heat source located behind another one due the increase in friction and form drags as illustrated in Fig. 14. However, installing single pair of rectangular winglets or groups in the vicinity of the stagnation zone between the heat sources has insignificant effect on the friction factor. The increase in the friction factor does not exceed 9.7% over $12{,}135 \leqslant Re_{Dh} \leqslant 34{,}305$ for all investigated configurations. The expected increase in the friction factor with VGs was not noticed due to the induced jet-like flow which reduces form drag that

opposes the increase in pressure drop due to the generated vortices. This result matches with Torii et al. [37] which provided that heat transfer enhancement is accompanied with pressure drop reduction for fin-tube heat exchangers with winglet type vortex generators (reached 53% reduction in the pressure drop).

5. Conclusions

An experimental investigation has been carried out to obtain heat transfer and pressure loss in a test section, simulated to in-lined two heat sources with common inflow rectangular winglet vortex generators. The effect spanwise and downstream distances, size, number and attack angle of vortex generator on the heat transfer rate and pressure drop were investigated in turbulent flow. The major conclusions from the present investigation are,

1. Attack angle of $\alpha = 45^\circ$ has better heat transfer enhancement for in-lined square heat sources with low height to length ratio ($\sim$1/5) for all investigated sizes and locations of the vortex generator.
2. Spanwise and downstream distances should also be optimized carefully to direct the flow into the core of the stagnation zone between heat sources. For in-lined square heat sources, the present study concluded that locating the vortex generator at downstream distance of (1/3–2/3)S and spanwise distance of (10/5–15/50)L have the largest heat transfer enhancement.
3. Vortex generator height of (3/4–3/2)B with length of (1/3–2/3)S gives better thermal performance with attack angle of $\alpha = 45^\circ$ due to the larger area facing the air flow and then the lower form drag and heat transfer enhancement. However, further study is needed for optimization.
4. In case of in-lined flat square heat sources, the heat transfer was augmented such Nu_L of the downstream heat source exceeds $Nu_{single\ heat\ source}$ by values reach 9.1% and 7.1% when installing G2, VG5 at $Re_L = 4676.2$, respectively. The drop Nu_L of the downstream heat source with VGs can be decreased to 8.% compared with 20.1% drop Nu_L without vortex generator within $8887 \leqslant Re_L \leqslant 12{,}929$.
5. An insignificant effect on the friction factor was obtained when installing a single pair or more of rectangular winglets in the vicinity of the stagnation zone. The increase in the friction factor does not exceed 9.7% over $12{,}135 \leqslant Re_{Dh} \leqslant 34{,}305$ for all investigated configurations.
6. This investigation showed that the applications of vortices generators in cooling of heat dissipation elements as an enhancement technique is promise, but deeper understanding of flow structure and optimizing vortex generator size for specific location and orientation is needed.

References

[1] R. Remsburg, Thermal Design of Electronic Equipment, second ed., CRC Press LLC, Boca Raton, FL, 2001.
[2] N. Sherwani, Q. Yu, S. Badida, Introduction to Multi-Chip Modules, third ed., John Wiley & Sons, New York, 1995.
[3] R.C. Chu, R.E. Simons, M.J. Ellsworth, R.R. Schmidt, V. Cozzolino, Review of cooling technologies for computer products, IEEE Trans. Device Mater. Reliab. 4 (4) (2004).
[4] R. Sedney, A survey of the effects of small protuberances on boundary layer flows, AIAA J. 11 (1973) 782–792.
[5] F.P. Incropera, Convection heat transfer in electronic equipment cooling, ASME J. Heat Transfer 110 (1988) 1097–1111.
[6] S. Sathe, B. Sammakia, A review of recent developments in some practical aspects of air-cooled electronic packages, ASME J. Heat Transfer 120 (1998) 830–839.
[7] A.E. Bergles, Evolution of cooling technology for electrical, electronic, and microelectronic equipment, IEEE Trans. (On Compon. Pack. Technol.) 26 (1) (2003) 6–15.
[8] J.R. Culham, P. Teertstra, M.M. Yovanovich, Thermal wake effects in printed circuit boards, J. Electron. Manufact. 9 (1999) 99–106.
[9] M. Faghri, M. Molki, Y. Asako, Air Cooling Technology for Electronic Equipment in Entrance Design Correlations for Circuit Boards in Forced Air Cooling, third ed., CRC Press LLC, Boca Raton, FL, 1996. pp. 47–80.
[10] R.A. Wirtz, Air Cooling Technology for Electronic Equipment in Forced Cooling of Low-Profile Package Arrays, second ed., CRC Press, Boca Raton, FL, 1996. pp. 81–101.
[11] E.M. Sparrow, J.E. Niethammor, A. Chaboki, Heat transfer and pressure drop characteristics of arrays of rectangular modulus encountered in electronic equipment, Int. J. Heat Mass Transfer 25 (1982) 961–973.
[12] E.M. Sparrow, S.B. Vemuri, D.S. Kadle, Enhanced and local heat transfer, pressure drop, and flow visualization, Int. J. Heat Mass Transfer 26 (1983) (1983) 689–699.
[13] E. Ratts, C.H. Ammon, B.B. Mikic, A.T. Patera, Cooling Technology for Electronic Equipment, Edited by Win Aung, Hemisphere Publishing Corporation, New York, 1988. pp. 183–194.
[14] G.E. Karniadakis, B.B. Mikic, A.T. Patera, in: Win Aung (Ed.), Heat Transfer Enhancement by Flow Destabilization: Application to the Cooling of Chips, Hemisphere Publishing Corporation, New York, 1988, pp. 587–610.
[15] J.H. Chou, J. Lee, in: Win Aung (Ed.), Cooling Technology for Electronic Equipment, Hemisphere Publishing Corporation, New York, 1988, pp. 113–124.
[16] H.W. Wu, S.W. Wang, S.W. Perng, The effective installation of an inclined plate for the enhancement of forced convection over rectangular sources, Heat Mass Transf. 33 (1998) 431–438.
[17] R.K. Ali, Heat transfer enhancement from protruding heat sources using perforated zone between the heat sources, Appl. Therm. Eng. 29 (2009) 2766–2772.
[18] R.K. Ali, Augmentation of heat transfer from heat source placed downstream a guide fence: an experimental study, Exp. Thermal Fluid Sci. 33 (2009) 728–734.
[19] L. Luviano-Ortiz, A. Hernandez-Guerrero, C. Rubio-Arana, R. Romero-Mendez, Heat transfer enhancement in a horizontal channel by the addition of curved deflectors, Int. J. Heat Mass Transfer 51 (2008) 3972–3984.
[20] C. Herman, E. Kang, Heat transfer enhancement in a grooved channel with curved vanes, Int. J. Heat Mass Transfer 45 (2002) 3741–3757.
[21] C. Herman, E. Kang, Comparative evaluation of three heat transfer enhancement strategies in a grooved channel, Heat Mass Transf. 37 (2001) 563–575.
[22] S. Ferrouillat, P. Tochon, C. Garnier, H. Peerhossaini, Intensification of heat transfer and mixing in multifunctional heat exchangers by artificially generated streamwise vorticity, Appl. Therm. Eng. 26 (16) (2006) 1820–1829.
[23] G. Zhou, Q. Ye, Experimental investigations of thermal and flow characteristics of curved trapezoidal winglet type vortex generators, Appl. Therm. Eng. 37 (2012) 241–248.
[24] S. Tiwari, D. Maurya, G. Biswas, V. Eswaran, Heat transfer enhancement in cross-flow heat exchangers using oval tubes and multiple delta winglets, Int. J. Heat Mass Transfer 46 (2003) 2841–2856.
[25] S. Jayavel, S. Tiwari, Effect of vortex generators and integral splitter plate on heat transfer and pressure drop for laminar flow past channel-confined tube banks, Heat Transfer Eng. 31 (5) (2010) 383–394.
[26] C.N. Lin, Y.W. Liu, J.S. Leu, Heat transfer and fluid flow analysis for plate-fin and oval tube heat exchangers with vortex generators, Heat Transfer Eng. 29 (7) (2008) 588–596.
[27] A.M. Jacobi, R.K. Shah, Heat transfer enhancement through the use of longitudinal vortices: a review of recent progress, Exp. Thermal Fluid Sci. 11 (1995) 295–309.
[28] S. Chomdee, T. Kiatsiriroat, Air cooling enhancement with delta winglet vortex generators in entrance region of in-line array electronic modules, Heat Transfer Eng. 28 (4) (2007) 372–379.
[29] R.A. Wirtz, P. Dykshoorn, Heat transfer from arrays of flat packs in channel flow, in: Proceedings of the Fourth International Electronic Package Society Conference, New York, 1984, pp. 318–326.
[30] E.M. Sparrow, A.A. Yanezmoreno, D.R. Otis, Convective heat transfer response to height differences in an array of block-like electronic components, Int. J. Heat Mass Transfer 27 (1984) 469–473.
[31] S.J. Kline, F.A. McClintock, Describing uncertainties in single-sample experiments, Mech. Eng. 75 (1) (1953) 3–8.
[32] B.A. Jubran, S.A. Swiety, M.A. Hamdan, Convective heat transfer and pressure drop characteristics of various array configurations to simulate the cooling of electronic modules, Int. J. Heat Mass Transfer 39 (16) (1996) 3519–3529.
[33] A.M. Anderson, R.J. Moffat, The adiabatic heat transfer coefficient and the superposition kernel function – I. Data from arrays of flat packs for different flow conditions, J. Electr. Pack. 114 (1992) 14–21.
[34] B.S. Petukhov, Heat Transfer in Turbulent Pipe Flow with Variable Physical Properties, Academic Press, New York, 1970.
[35] J.P. Holman, Heat Transfer, ninth ed., McGraw-Hill, New York, 2002.
[36] R. Kawai, K. Nishino, K. Torii, PIV measurement of 3-D velocity distribution around finned tubes with vortex generators, in: 4th International Symposium on Particle Image Velocimetry, Goettingen, September 17–19, 2001, p. 1100.
[37] K. Torii, K.M. Kwak, K. Nishino, Heat transfer enhancement accompanying pressure-loss reduction with winglet-type vortex generators for fin-tube heat exchangers, Int. J. Heat Mass Transfer 45 (2002) 3795–3801.